

## HIGH-ENERGY NUCLEAR-ACTIVE COMPONENT OF EXTENSIVE AIR SHOWERS AT SEA LEVEL

A. T. ABROSIMOV, V. A. DMITRIEV, G. V. KULIKOV, E. I. MASSAL'SKIĬ, K. I. SOLOV'EV, and G. B. KHRISTIANSEN

Nuclear Physics Institute, Moscow State University

Submitted to JETP editor September 15, 1958

J. Exptl. Theoret. Phys. (U.S.S.R.) **36**, 751-761 (March, 1959)

Data are presented on the number of high-energy nuclear-active particles in showers containing a total number of particles between  $1 \times 10^4$  and  $2 \times 10^6$ , and also on the lateral distribution of the energy flux of the nuclear-active component. It has been found that the energy of the nuclear-active component in individual showers with an equal number of particles may differ widely. Some conclusions are drawn from the shape of the spectrum of the nuclear-active particles and from the lateral distribution of the energy flux of the nuclear-active component regarding the nature of the elementary interaction of the nuclear-cascade process.

### INTRODUCTION

EXPERIMENTS on extensive air showers (EAS)<sup>1,2</sup> prove the presence of high-energy nuclear-active particles at sea level. The cascade of nuclear-active particles contained in EAS has, in the majority of past experiments, been studied indirectly by measuring the electron-photon and  $\mu$ -meson components accompanying the shower, or by methods which did not permit one to measure the energy of the nuclear-active particles directly.<sup>3</sup> The study of these cascades is of great interest in explaining the interaction process.

We carried out a statistical study of nuclear cascade in EAS at sea level, using a detector having a high efficiency for the detection of high-energy nuclear particles. The measurements were carried out in 1957, using the array for the comprehensive study of EAS operating at present at the Moscow State University.

### DESCRIPTION OF THE ARRAY\*

For the detection of nuclear-active particles and the determination of their energy, we used four cylindrical pulse ionization chambers placed under a composite absorber made of lead and graphite. The charged particles in EAS were recorded by 720 Geiger-Müller counters with different areas. The counters were connected to a hodoscope. The masterpulse for the chambers and the hodoscope was given by a six-fold coincidence of

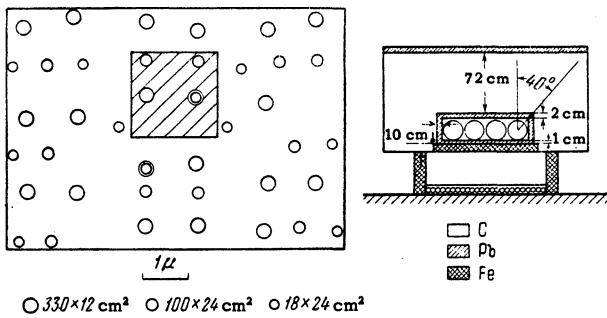
\*A detailed description of the apparatus and of the setup is given in references 2 and 4.

pulses from counter groups connected to a coincidence circuit. The area of each group amounted to  $330 \times 4 = 1320 \text{ cm}^2$ . The position of the chambers, the master counters, and a cross section of the detector are given in Fig. 1.

As has been mentioned,<sup>5</sup> the use of a composite absorber containing low-Z material (graphite) together with high-Z material (lead) makes it possible to separate, to a maximum extent, the nuclear and electron-photon cascades along the depth of the absorber. The development of the nuclear cascade takes place mainly in the graphite, while that of the electron-photon cascade takes place mainly in lead. In this way, an approximate proportionality of the number of particles in the electron-photon cascade to the energy carried away by  $\pi^0$  mesons is assured for any place of initiation of the nuclear cascade. In the study of showers of large size (with total number of particles  $N \geq 1 \times 10^5$ ) the thickness of the top layer of lead was increased to 8 cm since, in such showers, the frequency of incidence of electrons or photons with energies of about  $10^{11}$  ev on the array is high and the cascades produced by these particles are not fully absorbed by 4-5 cm lead.<sup>2</sup>

### RESULTS OF MEASUREMENTS

The selection system efficiently detected showers with  $N \geq 10^4$ . The spectrum of EAS selected by the array is the usual one for arrays of a similar type, with a maximum for  $N = 2.5 \times 10^4$ . The density of the distribution of the axes of registered showers was practically constant in a circle with radius 2.5 m for showers with  $N \geq 1 \times 10^4$ , and



○ 330×12 cm<sup>2</sup> ○ 100×24 cm<sup>2</sup> ○ 18×24 cm<sup>2</sup>

FIG. 1. Plan of the array and cross section through the detector.

the density of the axes of low-density showers fell off for large distances. For showers with  $N \geq 1 \times 10^5$ , the axes are distributed uniformly in a circle with radius  $R = 5$  m.

Reduction of the hodoscope data by the usual method<sup>6</sup> made it possible to determine, for each individual shower, the total number of particles  $N$  and the position of the axis. A part of the hodoscope data was reduced using an electronic computer, and in these cases, the method used was that of directly finding the probability maximum for a given distribution of discharged counters in all hodoscope points as a function of  $N$  and the position of the shower axis.<sup>7</sup> Thus, it was unnecessary to calculate the density of each hodoscopic point. A comparison of the characteristics of showers reduced by the usual method and by means of the computer shows, that the error in finding the shower axis in the first method was not greater than 1 m, while the error in the determination of the total number of particles was not greater than 20% (when the shower axis fell into the hodoscope area).

The chamber section records the amplitude of ionization bursts produced in the chambers when an EAS passes through the array. The size of the bursts is expressed in the number of  $N$  relativistic particles passing through the chamber along the mean chord. In order to obtain the energy of the nuclear-active particle from the burst size, we used the same coefficient for all energies of nuclear-active particles. The value of the coefficient is given in the appendix. The contribution of bursts from nuclear disintegrations and radiation bursts from  $\mu$ -mesons have been discussed earlier,<sup>5</sup> and were found to be insignificant.

All recorded and reduced showers were divided into four groups, according to the number of particles in the shower:

$$1 \cdot 10^4 \leq N_1 < 3 \cdot 10^4; \quad 3 \cdot 10^4 \leq N_2 < 1 \cdot 10^5;$$

$$1 \cdot 10^5 \leq N_3 < 3 \cdot 10^5; \quad N_4 \geq 3 \cdot 10^5.$$

To obtain more data we considered 218, 270, 186,

TABLE I. Number of particles with energy larger than a given value in a circle with radius  $R$  in showers of different size, and the maximum energy of nuclear-active particles detected in the shower

$E$ , ev	$R = 3$ m; $10^4 \leq N < 3 \cdot 10^4$	$R = 4$ m; $3 \cdot 10^4 \leq N < 10^5$	$R = 5$ m; $10^5 \leq N < 3 \cdot 10^5$	$R = 6$ m; $3 \cdot 10^5 \leq N < 2 \cdot 10^6$
$10^{11}$	2	7	29	55
$3 \cdot 10^{11}$	1.3	3	14	29
$10^{12}$	0.7	2.5	10	24
$2 \cdot 10^{12}$	0.1	0.7	2.5	9
$5 \cdot 10^{12}$		0.4	1.0	5
$7 \cdot 10^{12}$		0.2	0.8	3
$1.5 \cdot 10^{13}$			0.4	2
$5 \cdot 10^{13}$				1.0
$E_{na}^{max}$ , ev	$4.7 \cdot 10^{12}$	$10^{13}$	$1.8 \cdot 10^{13}$	$6 \cdot 10^{13}$

and 100 showers in each group respectively. Plots of the number of particles with energy greater than a given value were constructed for an average shower of each group. In fact, the number of recorded showers  $N(E)$  of each group accompanied by bursts of  $n$  particles, i.e., produced by a particle of energy  $E = kn$ , is related to the total number of showers  $N_s(\leq R)$  in a circle of radius  $R$  for a constant probability of shower detection, the axes of which fall within a circle with radius  $R$ , according to the formula

$$M(E) = \int_0^R \sigma \varphi(N) W(N, r) \rho(E, r) 2\pi r dr$$

$$= \sigma W \varphi(N) \int_0^R \rho(E, r) 2\pi r dr = \sigma N_s(\leq R) n(E) / S,$$

i.e.,

$$n(E) = M(E) S / N_s(\leq R) \sigma.$$

Here  $n(E)$  is the number of particles with energy  $E$  in the average shower in a circle with radius  $R$ ,  $r$  is the distance from the shower axis to the center of the detector,  $W$  is the probability of shower detection,  $\sigma$  is the detector area,  $\rho(E, r)$  is the density of particle energy  $E$  in the shower,  $\varphi(N)$  is the number of showers in the interval under consideration per unit area, and  $S = \pi R^2$ . The condition  $W = \text{constant}$  determines the choice of the radius of the circle for the construction of the spectra of particles (bursts), for different number of particles in the shower. For the groups mentioned above, the radii equal to 3, 4, 5, and 6 m respectively were chosen.\* The mean

\*It should be noted that the condition  $W = \text{constant}$  is satisfied in practice also for low-density showers, since the master counters are separated by a distance of about 2 m; the probability of recording such showers is smaller than unity, but its value does not change greatly. For a shower with  $N = 1 \times 10^5$ ,  $W$  changes in the chosen circle by 5%; for  $N = 2 \times 10^4$  by 30%. It can be shown easily that the errors introduced into the value of  $n(E)$  are smaller than the given change of  $W$ .

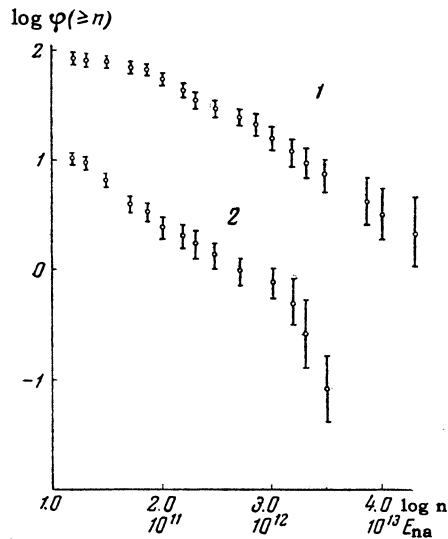


FIG. 2. Spectrum of nuclear-active particles in showers of different density: 1 – in showers with  $N = 5.6 \times 10^5$  ( $R \leq 6$  m); 2 – in showers with  $N = 2 \times 10^4$  ( $R \leq 3$  m).

number of particles with energy greater than a given value in the above-mentioned average shower of each group, obtained by means of the formula given above, is given in Table I. In Fig. 2, the integral spectra for the two limiting groups of showers are given. In the region  $E \geq 10^{12}$  ev, the spectra are characterized by different values of exponents: for  $N_1$   $\gamma = 1.8 \pm 0.5$ , for  $N_3$   $\gamma = 0.9 \pm 0.3$ , and for  $N_4$   $\gamma = 0.7 \pm 0.3$ . The spectrum of bursts in the same region for all showers with  $N \geq 1 \times 10^4$  is given in Fig. 3. In that case,  $\gamma = 1 \pm 0.2$ .

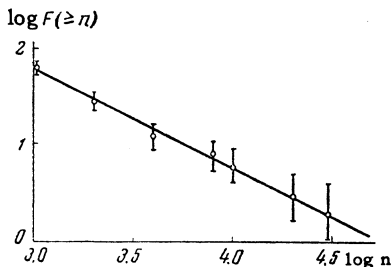


FIG. 3. Spectrum of large bursts ( $n \geq 1000$ ) in showers with  $N \geq 1 \times 10^4$ .

Data on the number of particles with a given energy  $n(E)$  in the average shower make it possible to determine the value of the total energy carried by the nuclear-active component of the shower in the circle of radius  $R$  ( $E_{na} = \sum n(E_i) \bar{E}_i$ , where the summation is carried out over all energy ranges). In Table II, these data are given for two groups of showers.\* When the position of the axis

\*The use, in the energy of estimates, of circles of larger radius for larger showers does not change the energy appreciably. Thus, the value of energy in the circle 4 m in radius for showers of the group  $N_3$  is different only by 4% from that given in Table II, and for showers in the group  $N_4$  by 5%.

and the size of the burst for each shower are known, it is possible to determine the lateral distribution of the energy flux carried by the nuclear-active component at the shower axis.

The energy flux density  $\rho_E(r)$  at the distance  $r$ ,  $r + \Delta r$  was determined from the formula

$$\rho_E(r) = \sum E_i / N_S(r) \sigma,$$

where the summation is carried out over all energy values recorded at the distance  $r$ ,  $r + \Delta r$ ;  $N_S(r)$  is the number of recorded showers whose axis fell between  $r$  and  $r + \Delta r$  from the detector. The distribution of energy density for separate groups of showers and for the average shower are given in Figs. 4 and 5.\*

Data were also obtained on the lateral distribution function of particles of various energies in showers. If  $m(r, n)$  out of  $N_S(r)$  showers whose axis fell between  $r$  and  $r + \Delta r$  were accompanied by a burst of  $n$  particles then, for  $\rho\sigma \ll 1$ ,

$$\rho(r, n) = m(r, n) / \sigma N_S(r),$$

where  $\sigma$  is the area of the detector, and  $\rho(r, n)$  is the particle density of a given energy. The experiment shows that  $m(r, n) \ll N_S(r)$  and, consequently, the formula is correct.

Figure 6 shows histograms for particles of various energies and also data obtained for particles with  $E_{na} \geq 8 \times 10^{11}$  ev in showers evaluated using the electronic computer. It should be noted that the maximum distance of particles with energy  $E_{na} \sim 10^{12}$  ev from the shower axis recorded by us corresponds to 5 m and, for showers with  $E_{na} \sim 10^{11}$  ev, to 30 m. This cannot be due to several particles of smaller energy, since the corresponding bursts were due to ionization in one chamber only.

## DISCUSSION OF RESULTS

Data on the spectra of nuclear-active particles given above show that the shape of the spectrum in various energy ranges is not the same for showers with different number of particles. For showers

\*Data on the lateral energy distribution make it possible to determine the energy flux carried by the nuclear-active component in another way:  $E'_{na} = \sum \rho_E(r_i) \Delta S_i$  where  $\Delta S_i$  is the area of the ring in which  $\rho_E(r_i)$  has been determined. Such a determination of  $E'_{na}$  is, in principle, less accurate, since the influence of the recorded individual value of the energy vary strongly for different ranges of  $r$  in the same shower. This process of axis translation takes place since the accuracy of determination of the axis is of the order of  $\sim 1 \text{ m} \sim \Delta r$ . The values of  $E'_{na}$  are given in Table II.

TABLE II. Values of the energy carried by the nuclear-active component in a circle with radius R in showers of different size

$N$	$10^4 \leq N < 3 \cdot 10^4$	$3 \cdot 10^4 \leq N < 10^5$	$1 \cdot 10^5 \leq N < 3 \cdot 10^5$	$3 \cdot 10^5 \leq N$
$E_{na}, \text{ ev}$	$(2.1 \pm 0.5) \cdot 10^{12}$	$(7.6 \pm 2.2) \cdot 10^{12}$	$(2.9 \pm 0.9) \cdot 10^{13}$	$(1.3 \pm 0.67) \cdot 10^{14}$
$E'_{na}, \text{ ev}$	$2.1 \cdot 10^{12}$	$8.0 \cdot 10^{12}$	$3.1 \cdot 10^{13}$	$6.3 \cdot 10^{13}$

of the group  $N_1$ , the region with an exponent  $\gamma > 1$  ( $\gamma = 1.8 \pm 0.5$ ) starts for the energy  $E_{na} > 10^{12}$  ev. (For showers of a smaller size, according to reference 2, for  $E_{na} \geq 10^{12}$  ev,  $\gamma = 1.5 \pm 0.2$ .) In the same energy range of nuclear-active particles ( $10^{12}$  ev  $\leq E_{na} \leq 10^{13}$  ev) and for showers with larger number of particles (group  $N_3$ ),  $\gamma = 0.9 \pm 0.3$ , and for showers of the group  $N_4$ ,  $\gamma = 0.7 \pm 0.3$ . The value  $\gamma \leq 1$  for showers with small number of particles of the group  $N_1$  corresponds to the energy region  $10^{11}$  ev  $\leq E_{na} \leq 10^{12}$  ev. Such a character of the energy spectra follows from the assumption that the nuclear cascade does not depend greatly on the energy. Several authors<sup>8</sup> assume that the character of the elementary interaction for the energies  $E \gtrsim 10^{14}$  ev changes abruptly. In order to test the effect of a change of the elementary interaction, as done by Nikol'skiĭ et al.,<sup>8</sup> we calculated the

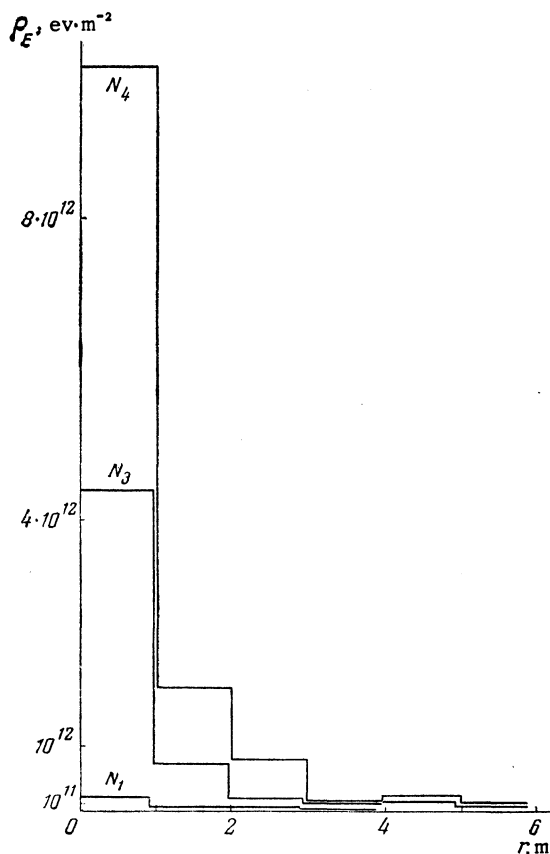


FIG. 4. Energy flux density of nuclear-active particles in showers with different  $N$ .

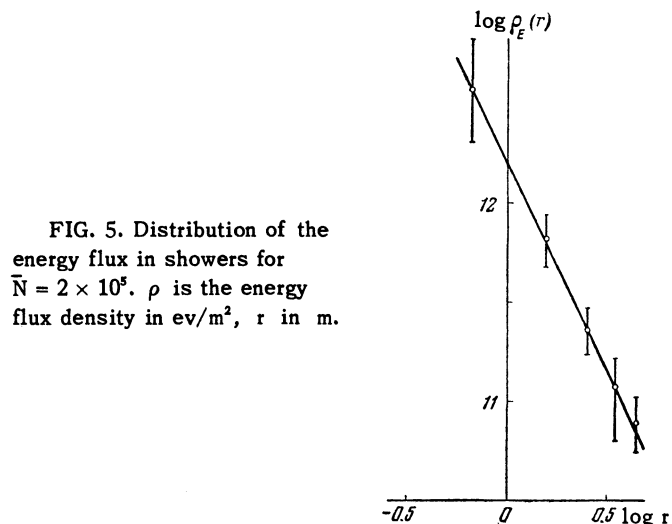


FIG. 5. Distribution of the energy flux in showers for  $\bar{N} = 2 \times 10^5$ .  $\rho$  is the energy flux density in  $\text{ev}/\text{m}^2$ ,  $r$  in m.

spectra of nuclear-active particles in showers with different initial energy ( $E_0 \sim 3 \times 10^{15}$  ev and  $E_0 \sim 3 \times 10^{14}$  ev) for constant characteristics of the interaction and for a sharp dispersal of the energy in interactions with  $E \geq 10^{14}$  ev. The calculation was done by the method of consecutive generations.<sup>9</sup> It was assumed, after Vernov et al.<sup>10</sup> that two particles with  $E = 0.3 E_0$  are produced in the interaction, and that, for  $E \geq 10^{14}$  ev, six particles with  $E = 0.1 E_0$  are produced. The calculations carried out under the assumption that the character of the interaction between particles does not vary with the particle energy, show that the mean exponent of the spectrum for showers of different size in the intervals  $10^{11}$  ev  $< E_{na} < 10^{12}$  ev and  $10^{12}$  ev  $< E_{na} < 10^{13}$  ev differ greatly (for  $E_0 = 3 \times 10^{15}$  ev,  $\gamma_1 = 0.9$ ,  $\gamma_2 = 1.1$ ; for  $E_0 \approx 3 \times 10^{14}$  ev,  $\gamma_1 = 1.1$ , and  $\gamma_2 = 1.4$ ). For the above variation of the character of the interaction, the spectra are very similar in both ranges ( $\gamma_1 = 1.1$ ,  $\gamma_2 = 1.4$ , and  $\gamma_1 = 1.2$ ,  $\gamma_2 = 1.5$  correspondingly). Such a result is natural: for rapid dispersal of the energy, the energy of nuclear-active particles becomes smaller than the "critical" energy ( $\leq 10^{14}$  ev) already after a small number of interactions. Further development of showers produced by primary high-energy particles then proceeds in the same way as for shower produced by particles of lower energies. The contribution of high-energy particles produced in the first interaction is small at sea level, in view of

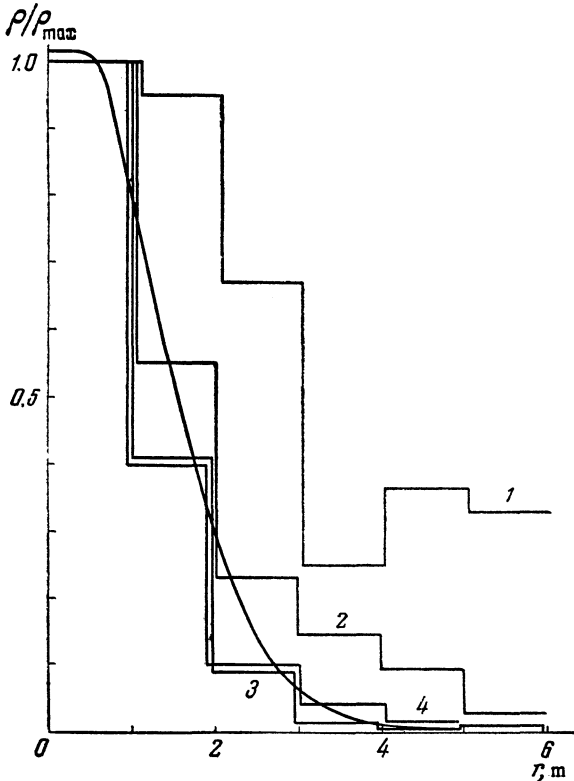


FIG. 6. Lateral distribution of nuclear-active particles in showers for particles with energy: 1 -  $1 \times 10^{11}$  to  $3 \times 10^{11}$  ev; 2 -  $3 \times 10^{11}$  to  $1 \times 10^{12}$  ev; 3 -  $\geq 1 \times 10^{12}$  ev; 4 - data for particles with  $E \geq 8 \times 10^{11}$  ev calculated with an electronic computer.

the large depth of the observation level. Therefore, the result will be the same for any other assumption concerning the character of the interaction, if only we assume a strong degeneration of energy for energies higher than a certain "critical" value.

The comparison of the experimental data with the calculation shows that the assumption about an abrupt change of the elementary interaction for  $E \geq 10^{14}$  ev is unnecessary, and indicates rather a weak dependence of the characteristics of the elementary act of interaction on the energy. For a final solution of this problem, more accurate data in the range of large energies of  $E_{na}$  are necessary.

As may be seen from Table II, the value of the energy carried out by the nuclear-active component in the average shower is of the order of the energy carried by the electron-photon (e.p.) component of the shower, and is proportional to shower size, at least in the range of  $N$  from  $1 \times 10^4$  to  $1 \times 10^6$  (energy of the e.p. component  $E_{ep} \approx 3\beta N \approx 2 \times 10^8 N$  ev). The values given in the table represent the lower estimate of the energy carried by the nuclear-active component of the shower. In fact, in the showers with  $N \geq 1 \times 10^4$ , the spectrum of

nuclear-active particles has been studied by us up to the energy range where the spectrum exponent  $\gamma$  is of the order of 1. On the other hand, we took into account the energy of the nuclear-active component in the circle with radius 6 m, where the gradient of the lateral distribution function of the energy flux is of the order of  $\sim r^{-2}$  (see below). It is therefore possible in principle, that we did not take into account a part of the energy of the nuclear-active component.

The presence of such energy in the nuclear-active component at the observation level can substantially change the absorption of the shower particles. The variation of the energy of the electron-photon component in a layer with thickness  $dt$  is given by the equation

$$dE_{ep} = -\beta N dt + (1 - \alpha)(t_0/\lambda) E_{na} dt,$$

where  $(1 - \alpha)$  is the energy fraction carried away by  $\pi^0$  mesons in nuclear interactions,  $E_{na}$  - the energy carried by the nuclear-active component,  $t_0$  - the radiation length in  $g/cm^2$ , and  $\lambda$  - the mean free path for nuclear interactions in  $g/cm^2$ . In the electron-photon cascade for  $1.5 \geq s \geq 1.2$ , the mean energy  $\bar{\epsilon}$  per charged particle is practically independent of  $s$ ,<sup>11</sup> and therefore:

$$\bar{\epsilon} dN = -\beta N dt + a E_{na} dt.$$

The solution of this equation can be obtained easily if the absorption of the energy of the nuclear-active component in the atmosphere is known. Assuming that  $E_{na} = E_0 \exp(-\mu_n t)$  where  $\mu_n$  is the absorption coefficient of the energy of nuclear-active component in the air, and  $E_0$  is the energy of the nuclear-active component at the observation level, we obtain for (for  $\mu_0 > \mu_n$ )

$$N(t) = \left[ N_0 - \frac{a E_0}{\bar{\epsilon}(\mu_0 - \mu_n)} \right] e^{-\mu_0 t} + \frac{a E_0}{\bar{\epsilon}(\mu_0 - \mu_n)} e^{-\mu_n t},$$

where  $N_0$  is the number of particles in the shower at the observation level, and  $\mu_0$  is the absorption coefficient of particles in showers for  $E_{na} = 0$ . The number of shower particles absorbed at large depths is determined by the absorption of the energy of the nuclear-active component. As can be seen from the expression obtained, the development of the shower with a given  $N$  is substantially dependent on the value of the energy  $E_0$  of the nuclear-active component of the shower. Near the observation level, the absorption is characterized by the absorption coefficient

$$\mu = \mu_0 - a E_{na} / E_{ep}; \quad \Delta\mu = \mu_0 - \mu = a E_{na} / E_{ep}.$$

The absorption coefficient of shower particles is  $\mu = 0.17$ .<sup>3</sup> For  $(1 - \alpha) = 0.3$  and  $E_{na} / E_{ep} = 1.0$ ,

we have  $\Delta\mu = 0.05$ ; for  $(1 - \alpha) = 0.1$ ,  $\Delta\mu = 0.08$ . The measured values of the coefficient  $\mu_0 = 0.22 - 0.25$ , correspond to  $s = 1.3$ .<sup>12</sup>

Data on the average number of nuclear-active particles of various energies in showers of different size show that, in certain showers, we recorded nuclear-active particles of such energies that the mean frequency per shower was less than unity. The energy of single particles recorded in the first group of showers is equal to the total energy carried by the electron-photon component of such a shower. The exponent of the energy spectrum in this energy region for showers with  $N \geq 3 \times 10^4$  is  $\gamma \leq 1$ , and, consequently, the total energy of the nuclear-active component in such showers is large ( $E_{na} \gg E_{ep}$ ). This indicates a strong variation of the absorption coefficient  $\mu$  in the shower.

In showers of small size,  $N \leq 1 \times 10^4$ , we recorded<sup>2</sup> showers with the measured energy of nuclear-active component larger by a factor of 10 than the energy of the electron-photon component. In such showers, one would expect a further increase in the number of particles rather than their absorption.

The fact that in individual showers, nuclear-active particles are present with an energy much larger than the average energy of particles which are found in each shower indicates strong fluctuations in shower development. This conclusion, drawn in reference 2 for showers with small number of particles, is correct for showers with  $N < 3 \times 10^5$ . Insufficient statistics does not permit to make an analogous conclusion for showers with  $N > 3 \times 10^5$ .

The large fluctuations in the energy balance of the showers, the energy carried by the nuclear-active component may be much lower than the average. In the limiting case, (for  $E_{na} = 0$ ), the absorption of particles in showers is determined by  $\mu_0$ . It should be noted that the detection of such showers is possible from a study of the energy balance of the different components in the shower core, since the difference in the lateral distribution of the particle flux due to different shower age may be insufficient for determining the age in individual showers by means of the method of correlated hodoscopes.

At the same time, it should be noted that, the observed value of the energy of the nuclear-active particles in the average shower confirms the limiting assumption about the relation between the nuclear-active and the electron-photon shower components (i.e., that on the average, an equilibrium exists between the nuclear-active and

electron-photon components). In reference 1, the energy of the nuclear-active components was estimated for such a case. The relation which was obtained, namely  $E_{na} \approx 10^8 N$  ev, is satisfied for all  $N$ , as can be seen from Table II. Data on the energy composition of showers obtained at mountain altitudes<sup>13</sup> indicate also that the nuclear component plays a large role. The conservation of the relative contribution of the energy carried in the shower by the different components at two altitudes also confirms the assumption that, on the average, the two components are in equilibrium.

The obtained lateral distribution of the energy flux of nuclear-active component in showers with given  $N$  (Fig. 5) can be well approximated by a power law with an exponent  $n = 2 \pm 0.4$ , apart from the dependence on the shower size.\*

Recently various authors<sup>14</sup> have obtained data showing that the transverse momentum of particles produced in nuclear interactions is independent of the energy carried away by the particle. This fact can be used to obtain the lateral distribution of the energy flux of nuclear-active particles. We carried out such a calculation in which we used the method of consecutive generations, in order to obtain the energy spectrum of particles produced in interactions. We used very simple models of the interactions, following reference 10. From the same work we took also the values of the mean free path for the interactions for various models, obtained from the normalization to the observed number of particles with energy greater than a given value in a shower at sea level. The mean production level for particles of each generation was introduced. It was assumed that the particles of given energy are distributed uniformly in a circle, the mean radius of which is determined from the value of the particle energy and the level of production. The transverse momentum, according to our estimates (see below) and estimates of reference 14, is assumed to be equal to  $10^9$  ev/c. The atmosphere was assumed to be homogeneous, since the production level of particles which are essential to the discussion was not greater than one third of the atmosphere.

The obtained lateral distribution of the energy flux, was, for the same transverse momenta, found to be sensitive to the type of interaction. For distances of 0.5 — 8 m, the lateral distribution can be

\*Lateral distribution of the energy flux of the nuclear-active component averaged over showers with  $N = 1 \times 10^4 - 2 \times 10^6$  is characterized by an exponent  $n = 2 \pm 0.25$ .

described by a power law with exponent  $n$ , where  $n$  depends on the model of interaction:

If 7 particles with energy	$0.1 E_0$	are produced,	then	$n = 1.8$
" 2 "	" "	" "	" "	" $n = 2.1$
" 1 "	" "	" "	" "	" $n = 2.4$
" 1 "	" "	" "	" "	" $n = 2.4$

An even sharper difference is observed for  $r > 10$  m. These distances, however, were not investigated in our work. A comparison of the experimental data with the calculations shows that, for the accuracy attained, a final unambiguous conclusion on the shape of the function of the lateral energy distribution cannot be drawn.

The data of Fig. 6 show a sharp concentration of particles of high energies ( $E \approx 10^{12}$  ev) near the shower axis. For the estimate of the width of the distribution of high-energy particles, a calculation of the lateral distribution of shower axes in the plane of hodoscope counters was carried out, based on the following assumptions: (1) the accuracy of axis location by means of hodoscope counters is  $\pm 1$  m, and the fluctuations are subject to the Gauss distribution law, (2) the zenith-angle distribution of shower axes is given by the relation  $I(\theta) = I_0 \cos^8 \theta$ , (3) nuclear-active particles of high energies are concentrated near the shower axis.

The area of the chamber amounts to  $\sigma = 1 \text{ m}^2$ , and the height of the counter plane above the chamber  $h = 2$  m. The curve obtained as a result of the calculation, which reduces to a numerical integration of the Bessel function  $I_0(x)$ , is shown in Fig. 6 (solid line).

It can be seen from a comparison of the calculated results with the experimental data that the high-energy particles ( $E_{na} \geq 10^{12}$  ev) are concentrated in a narrow region around the shower axis, of the order of the size of the chamber ( $r \approx 1.0$  m). Particles with energy  $1 \times 10^{11} - 3 \times 10^{11}$  ev are distributed much more widely: their density at the distance of 6 m falls off only by a factor of three as compared with the central region.

The lateral distribution of particles with  $E \geq 10^{12}$  ev makes it possible to estimate the value of the transverse momentum obtained by such particles during their production. Assuming a height of production of  $\sim 2\lambda_{\text{inter}} \sim 10^3$  m, we obtain  $p_{\perp c} \leq 10^{12} \times 10^{-3} = 10^9$  ev.

In conclusion, the authors would like to express their gratitude to S. N. Vernov, and G. T. Zatsepin for their great help in the carrying out of the work and for helpful advice in discussing the results, and to G. V. Bogoslovskii, V. I. Artemkin, and V. N. Sokolov, who took part in the measurements.

## APPENDIX

### CONNECTION BETWEEN THE SIZE OF THE BURST AND THE MEAN VALUE OF THE PRIMARY-PARTICLE ENERGY

In references 2 and 5, we obtained the value of the coefficient relating the number of particles in the burst to the energy of the particle producing the burst, by means of an actual analysis of the interaction of the first four generations of a nuclear cascade in the absorber. The connection between the average energy carried away by mesons and the energy of the primary particle can also be found from energy considerations. In fact, the variation of the energy flux  $E_{\pi^0}(x)$  carried by the  $\pi^0$  mesons at the depth of the absorber  $x$  (in nuclear units) is described, if we neglect the  $\pi \rightarrow \mu$  decay, by the equation

$$dE_{\pi^0}(x)/dx = \beta(1 - \alpha)E_N(x) + \beta E_{\pi^\pm}(x),$$

where  $E_N(x)$  is the energy carried by nucleons at the depth  $x$ ,  $E_{\pi^\pm}(x)$  is the same for  $\pi^\pm$  mesons,  $\alpha$  is the energy fraction conserved by nucleons in interaction, and  $\beta$  is the energy of  $\pi^0$  mesons compared with the energy transferred to  $\pi$  mesons in the interaction.

Analogous equations determine the absorption of the energy carried by the nucleons and  $\pi^\pm$  mesons. The solution for the equation for  $E_{\pi^0}(x)$  is

$$E_{\pi^0}(x) = \left[ 1 - \frac{\alpha\beta}{\alpha + \beta - 1} e^{-(1-\alpha)x} + \frac{(1-\alpha)(1-\beta)}{\alpha + \beta - 1} e^{-\beta x} \right] E_N^0,$$

where  $E_N^0$  is the energy of the nucleon incident on the absorber. Assuming, after reference 15,  $\alpha = 0.7$  and  $\beta = 1/3$ , we obtain for  $x = 1.5$ ,  $E_{\pi^0}(1.5) = 0.18 \times E_N^0$ , and for  $x = 2$ ,  $E_{\pi^0}(2) = 0.25 \times E_N^0$ . The value  $x = 2$  corresponds to an absorber with 8 cm of lead over the graphite. In collision with the lead nucleus, a larger fraction of the energy is carried away by the mesons ( $\alpha < 0.7$ ),<sup>17</sup> but, in that case, a strong development of the electron-photon cascade from  $\pi^0$  occurs in the lead, and only a small part of the cascade energy reaches the lower layer of lead. We can therefore assume, to a first approximation, that the relations between the burst size and the energy of the primary particles, taking account of these interactions, will not change greatly. The development of a cascade in the lower layer of lead was considered on the basis of the data of Ivanenko.<sup>16</sup> Since the spectra of secondary  $\pi^0$  mesons are not known, average values were taken from the number of particles under lead, obtained

under the assumption that the cascade is due to one  $\pi^0$  meson with energy  $E_{\pi^0}$ , or to 10 mesons with energies  $0.1 E_{\pi^0}$  (the difference between these numbers amounts to about 20% for an energy  $E_{\pi^0} \sim 10^{10}$  ev). The value obtained for the coefficient is  $k = 7 \times 10^8$  ev for  $E_N^0 \sim 5 \times 10^{11}$  ev, and it increases slowly with the energy. If we assume that the energy is carried by a small number of high-energy  $\pi^0$  mesons, then for  $E_N^0 \sim 4 \times 10^{12}$  ev we have  $k = 2 \times 10^9$ . However,  $\pi^0$  mesons produced in the secondary interactions of  $\pi^\pm$  mesons have, on the average, an energy smaller by an order of magnitude than that of the  $\pi$  mesons produced in the interactions of the primary nucleon, and the energy fraction carried by them is insignificant. Taking this fact into account leads to a slower change of  $k$  with energy.\* For  $E_N^0 \sim 4 \times 10^{12}$  ev, we obtained the value  $k = 1.3 \times 10^9$  ev. In the following discussion we used the mean value of the coefficient  $k = 1 \times 10^9$  ev.

<sup>1</sup>Abrosimov, Goryunov, Dmitriev, Solov'eva, Khrenov, and Khristiansen, J. Exptl. Theoret. Phys. (U.S.S.R.) **34**, 1077 (1958), Soviet Phys. JETP **7**, 746 (1958).

<sup>2</sup>Dmitriev, Kulikov, and Khristiansen, J. Exptl. Theoret. Phys. (U.S.S.R.) (in press), Soviet Phys. JETP (in press).

<sup>3</sup>K. Greisen, Progress in Cosmic Ray Physics, Vol. III, Amsterdam (1956).

<sup>4</sup>Bekkermann, Dmitriev, Molchanov, Khristiansen, and Yarygin, Приборы и техника эксперимента (Instruments and Meas. Eng.) No. 4, (1958).

<sup>5</sup>Dmitriev, Kulikov, and Khristiansen, Suppl. Nuovo cimento **2**, 587 (1958).

\*For this purpose we solved the equations for the energy directly transferred to  $\pi^0$  mesons in interactions of the nucleon, and also in interactions of secondary  $\pi^\pm$  mesons.

<sup>6</sup>G. B. Khristiansen, Dissertation, Phys. Inst. Acad. Sci. 1953.

<sup>7</sup>G. V. Kulikov and G. B. Khristiansen, J. Exptl. Theoret. Phys. (U.S.S.R.) **35**, 625 (1958), Soviet Phys. JETP **8**, 44 (1959).

<sup>8</sup>Nikol'skii, Vavilov, and Batov, Dokl. Akad. Nauk SSSR **111**, 71 (1956), Soviet Phys. "Doklady" **1**, 625 (1956).

<sup>9</sup>G. T. Zatsepin and I. L. Rosental, Dokl. Akad. Nauk SSSR **99**, 369 (1954).

<sup>10</sup>Vernov, Gorchakov, Ivanenko, and Khristiansen, J. Exptl. Theoret. Phys. (U.S.S.R.) (in press), Soviet Phys. JETP (in press).

<sup>11</sup>I. P. Ivanenko, J. Exptl. Theoret. Phys. (U.S.S.R.) **35**, 132 (1958), Soviet Phys. JETP **8**, 94 (1959).

<sup>12</sup>S. E. Belen'kiĭ, Лавинные процессы в космических лучах (Cascade Processes in Cosmic Rays), M-L 1948.

<sup>13</sup>Dovzhenko, Zatsepin, Murzina, Nikol'skiĭ, and Rakobol'skaya, Dokl. Akad. Nauk SSSR **118**, 899 (1958), Soviet Phys. "Doklady" **3**, 122 (1958).

<sup>14</sup>G. L. Milekhin and I. L. Rozental', J. Exptl. Theoret. Phys. (U.S.S.R.) **33**, 197 (1957), Soviet Phys. JETP **6**, 154 (1958). Birger, Grigorov, Guseva, Zhdanov, Slavatinskiĭ, and Stashkov, J. Exptl. Theoret. Phys. (U.S.S.R.) **31**, 971 (1956), Soviet Phys. JETP **4**, 872 (1957); G. B. Zhdanov, J. Exptl. Theoret. Phys. (U.S.S.R.) **34**, 856 (1958), Soviet Phys. JETP **7**, 592 (1958).

<sup>15</sup>I. L. Grigorov, Usp. Fiz. Nauk **58**, 599 (1956).

<sup>16</sup>I. L. Ivanenko, Dokl. Akad. Nauk SSSR **107**, 819 (1956), Soviet Phys. "Doklady" **1**, 231 (1956).

<sup>17</sup>Grigorov, Podgurskaya, Savel'eva, and L. M. Poperekova, J. Exptl. Theoret. Phys. (U.S.S.R.) **35**, 3 (1958), Soviet Phys. JETP **8**, 1 (1959).